# Estimation of Cardiac Conduction Velocities Using Small Data Sets

TN Fitzgerald[1], EK Rhee[2], DH Brooks[3], JK Triedman[2]

[1] Department of Biomedical Engineering, Boston University, Boston, MA, USA
[2] Department of Cardiology, Children's Hospital, Boston, MA, USA
[3] Department of Electrical Engineering, Northeastern University, Boston, MA, USA

## Abstract

*Cardiac conduction velocities can provide information about both the speed and angle of a propagating electrical wavefront. Catheter based vector mapping may improve the visualization of cardiac arrhythmias, but catheters can only provide limited data. We address the problem of estimating conduction speed and angle from small data sets suitable for recording from a catheter device. We estimated cardiac conduction velocities using data subsets of 4 – 7 electrograms, and then compared the estimates to a larger reference grid. From 6 swine hearts, we studied 137 ventricular beats and 17,756 velocity vectors. Angle errors were 0.4° ± 16° and speed errors were 5% ± 33%. These initial data suggest that the signal processing required for catheter-based vector mapping is feasible.*

## 1. Introduction

Arrhythmias remain difficult to treat because cardiac electrical activity is difficult to visualize. Conduction velocity is used to characterize myocardial tissue in research and clinical applications. Catheter-based velocity vector mapping might improve the visualization of cardiac arrhythmias by providing information about both the speed and direction of electrical activity. However, the dimensions of a velocity vector mapping array would be stringently limited by catheter tip size.

Assuming a planar wavefront, Horner *et al* [1] designed a catheter containing 3 electrodes to measure conduction velocities *in vivo*. Bayly *et al* [2] estimated cardiac conduction velocities using an electrode grid. Spatial coordinates of the electrodes and activation times of the electrograms were used to construct a polynomial surface of cardiac activation, from which velocity vectors were calculated. The large numbers of electrodes used created an over-determined system and a reliable estimate, but cannot be realized as a catheter based device.

We estimated cardiac conduction velocities using small data sets from data obtained *in vitro* from swine right ventricle. Electrode arrays were chosen to fit the dimensions of a 2.5mm catheter tip. Velocity vectors from subsets were compared to the vector field estimated from larger data sets (24-56 electrodes) to assess the accuracy of the technique in the animal model.

## 2. Methods

### 2.1. Experimental procedure

The Animal Care and Use Committee of Children's Hospital approved animal use. Six swine (~10 Kg) were anesthetized and their hearts quickly removed and placed in modified Tyrode's solution (40mM KCl) at 0 °C. The free wall of the right ventricle (RV) was dissected to allow the right coronary artery to be cannulated and perfused with gassed (95% $O_2$, 5% $CO_2$) Tyrode's solution [3] at 32 – 36°C. The RV was paced from multiple locations.

A 5 x 6 mm array of 56 Ag/AgCl electrodes [4] was used to obtain unipolar electrograms from the epicardial surface (semi-uniform spacing, interelectrode distance: 690±80 μm). Signals were acquired at sample rate 1000Hz and band-pass filtered (30–500 Hz) to simulate clinical practice. The electrode array was rotated between electrogram recordings so that multiple wavefront angles could be studied. Procainamide (10 – 20 μg/ml) was used to slow conduction so that a range of speeds was obtained.

### 2.2. Signal processing

Pacing artifacts were excluded and velocities were calculated from a single beat. Each data set was digitally notch filtered at 60 and 180Hz. Given reported cardiac conduction as high as ≈ 1 m/s [2,6] and our mean electrode spacing of 0.69 mm, time delays significantly <1ms were expected. With a sampling frequency of 1000Hz, such delays could not be calculated using cross-correlation alone. A Hilbert transform was used to

interpolate the cross-correlation function, allowing small time delays to be detected [5]. The time delay estimate was taken as the point at which the Hilbert transform crossed the time axis, determined by linear interpolation.

## 2.3. Reference velocity calculation

Reference velocities were calculated using data from the entire grid (24-56 electrodes). The data was fit to a biquadratic polynomial surface similar to that used by Bayly *et al* [2]:

$$(T_2 - T_1) = a(X_2^2 - X_1^2) + b(Y_2^2 - Y_1^2) + c(X_2Y_2 - X_1Y_1) + \ldots$$
$$\ldots + d(X_2 - X_1) + e(Y_2 - Y_1). \quad (2)$$

X and Y are the Cartesian coordinates of 2 electrodes, $T_2$–$T_1$ is the time delay between the electrograms, and a-e are the parameters to be estimated.

Electrograms with signal-to-noise ratio < 2 were excluded. With 56 electrodes, over 1000 electrogram comparisons can be made. Only electrogram pairs with high maximum cross-correlation coefficients (MCCCs) were used in the estimator. Between 50 and 300 time delays were used to estimate the parameters, chosen in order of MCCCs. Ordinary least squares (OLS) was used to estimate the parameters a–e. Once the parameters were estimated, the reference velocity vector field was derived.

## 2.4. Subset velocity calculation

The signal processing algorithms in this study made 3 assumptions:

1. The activation wavefront approximates a plane wave over a region 2.5 mm in diameter.
2. Closely-spaced electrograms are sufficiently similar in waveshape to find delays by cross-correlation.
3. The spatial coordinates of the electrodes are precisely known (X and Y are noise free).

Velocities were calculated from small subsets (4 – 7 electrodes) of the larger grid. Subset arrays were chosen so that all electrodes fit into a circle of diameter 2.5 mm. The time delays between 2 electrograms ($T_2 - T_1$) and Cartesian coordinates (X,Y) of the electrodes were fit to the following model using OLS:

$$(T_2 - T_1) = a(X_2 - X_1) + b(Y_2 - Y_1) \quad (3)$$

# 3. Results

Unipolar electrograms (Figure 1) from 137 ventricular beats were analyzed. Velocity vectors for 17,756 subsets were calculated and compared to the corresponding reference vectors. We assumed that the reference model represented a gold standard velocity vector field, although we found this assumption was not true in several data sets. Therefore, we divided data sets into 2 groups: "well-behaved" and "poorly-behaved" velocity fields. In well-behaved velocity fields, angle and speed error ($\phi_A$ & $\phi_S$) were defined as follows:

$$\phi_A = \text{Reference Angle} - \text{Subset Angle} \quad (4)$$
$$\phi_S = (1 - \text{Subset Speed/Reference Speed}) * 100\% \quad (5)$$

## 3.1. Well behaved velocity fields

Velocity fields were defined as well-behaved if a single wavefront passed smoothly over the electrode grid and was accurately represented by the reference model. Figure 2 shows an example of a well-behaved velocity field. Isocontour activation maps were constructed according to the time of the minimum derivative in each electrogram. The contour suggests that a single wavefront passed from the left side of the electrode grid and disappeared into the upper right corner. The corresponding velocity vector field was calculated from the reference model, and agrees with the isocontour map.

Data sets from 65 ventricular beats were classified as well-behaved and 6607 velocity vector comparisons were made. Angle errors were 0.4° ± 16°. Speed errors were 5% ± 33%.

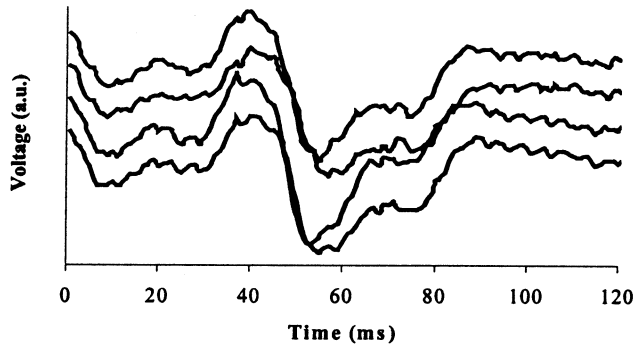

Figure 1. Electrograms collected from swine RV.

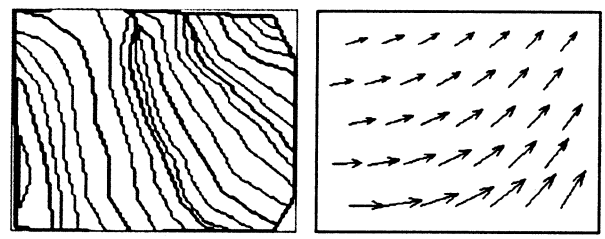
Figure 2. Well-behaved velocity field. Isocontour lines of minimum electrogram derivatives (left) and the reference velocity vector field (right).

Velocity estimates were made for subsets of 4,5,6 and 7 electrodes. When subsets of 7 were compared to subsets of 4, the standard deviations of the angle and speed errors only improved by 3° and 7% respectively (change in variance was statistically significant with $\alpha$=0.99).

A second example of a well-behaved velocity field is shown in Figure 3. Angle errors were 2.0° $\pm$ 35° and speed errors were 13% $\pm$ 75%, making this one of the worst members of the well-behaved velocity fields. However, one can still gain a sense for the overall pattern of cardiac activation by looking at the subset velocity field even in the presence of large errors.

## 3.2. Validation of assumptions

To investigate the assumption that closely-spaced electrograms would be similar in waveshape, we examined MCCCs as a function of interelectrode distance for a single beat (Figure 4). Electrodes separated by <1mm yielded the highest MCCCs (0.97 $\pm$ 0.03), but many electrodes separated by 5-6mm still yielded MCCCs > 0.90. Therefore, over the area of a catheter tip, electrograms are likely to be very similar in waveshape.

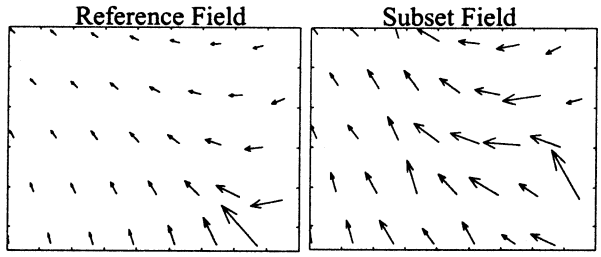


Figure 3. A well-behaved velocity field with large errors in the subset field.

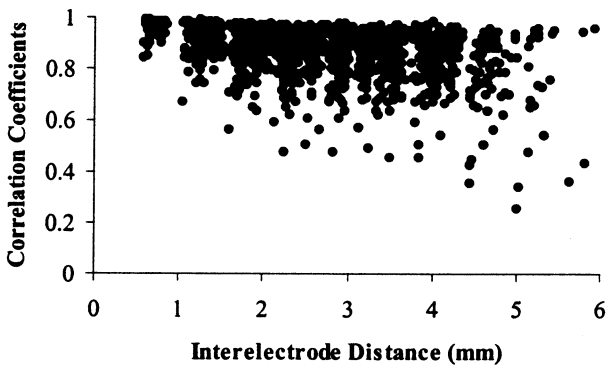


Figure 4. Maximum cross-correlation coefficients between electrograms in a single right ventricular beat.

We assumed that the activation wavefront could be modeled as planar over a region 2.5mm in diameter. Radii of curvature were determined for 2.5mm sections of the reference grid. Velocity errors did not change as a function of the radius of curvature, even for small radii.

## 3.3. Poorly behaved velocity fields

An example of a poorly behaved velocity field is shown in figure 5. The contour plot shows that the activation wavefront entered the lower edge of the grid in a well-behaved fashion, but then turned in the upper right corner. The velocity field derived from the reference model did not adequately represent the complexities of the activation pattern, but the velocity field derived from the subset model captured the important features of this complex rhythm.

# 4. Discussion

## 4.1. Examination of assumptions

The use of cross-correlation implied that signals were similar enough in waveshape that derived time delays could accurately predict velocity. We did not directly measure the accuracy of time delays *versus* MCCCs, but we did note that the derived velocities were more variable for MCCCs <0.90. Such MCCCs were most often seen for electrogram pairs separated by $\geq$ 2.5mm. Thus, the validity of this technique depended upon the similarities in electrogram morphology most often associated with proximity, and electrograms collected within the space of a catheter tip are likely to be similar.

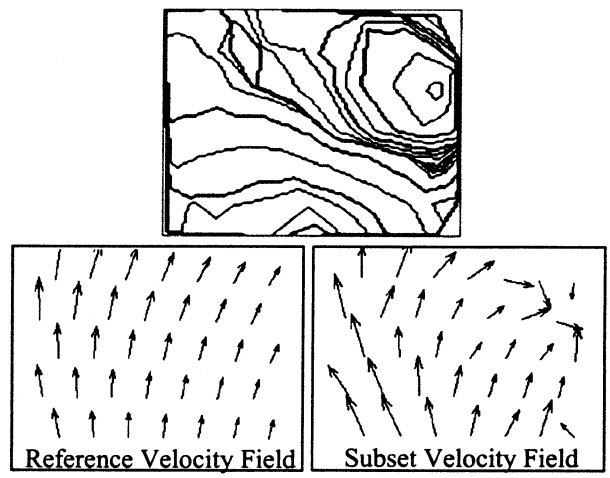


Figure 5. Poorly-behaved velocity field. Isocontour lines (top), reference velocity field (left) and subset velocity field (right).

We assumed that the activation wavefront could be modeled as planar over the region of the catheter tip. A polynomial with sufficient degrees of freedom to model curvature was not feasible given the statistical constraints of small data sets. Given velocity fields observed from the larger arrays and properties of myocardium [7], a linear model is reasonable in the area of the catheter tip. We tested this assumption and found that velocity errors did not changed as a function of radius of curvature.

### 4.2. Velocity accuracy

Accuracy of velocity estimates is dependent on underlying accuracy of the estimated time delays obtained from the raw signals. We did not measure time delay accuracy experimentally, but infer it from errors in velocity estimation. Velocity estimates can be improved by increasing the time delay accuracy.

We observed that velocity errors decreased by increasing the number of electrodes from 4 to 7 in an array. However, the standard deviation of the angle and speed errors only improved by 3° and 7% respectively. Although this improvement was statistically significant, it may not be sufficient to warrant a 2-fold increase in processing time and electrode fabrication.

It seems likely that angle estimates will be more important than speed estimates in creating a map of cardiac activation. Allowable angle and speed errors may depend on several factors such as: specific clinical application, spatial complexity of the arrhythmia, number of velocity vectors that can be obtained, stability of the arrhythmia and, in the end, subjective opinion of the user.

We obtained small velocity errors and demonstrated that even in the presence of large velocity errors (Figure 3) activation patterns could be recognized. Furthermore, we observed that small electrode subsets were able to capture important features of cardiac activation that were not adequately represented by the reference model. Both the reference and subset models induced smoothing. The reference model was unable to capture these important features because the smoothing was performed over the entire area of the electrode grid. The subset model only smoothed data within a diameter of 2.5mm.

### 4.3. Future work in vector mapping

These estimates were obtained using standard filtering and sampling techniques present in an electrophysiology workstation, and may be insufficient for cardiac vector mapping. Electrograms can contain frequencies up to and beyond 1000 Hz [8], and sampling at higher frequencies may add accuracy to time delay calculations. Other algorithmic enhancements that may reduce error include de-noising of electrograms without changing the phase of the signal and using data from multiple beats. The consequences of poor electrode-tissue contact and a catheter tip that does not rest perpendicular to the tissue must also be investigated.

## 5. Conclusion

Cardiac conduction velocities were estimated in swine right ventricle using small data sets (4 – 7 electrodes). Subset velocities adequately represented simple activation patterns that were described well by a biquadratic reference model, and were able to capture important features of complex cardiac activation when the reference model failed. These data suggest that catheter-based vector mapping is feasible from a signal processing point of view and provide a starting point for the development of cardiac vector mapping algorithms.

## Acknowledgements

This work was supported in part by a grant from Biosense Webster, Inc. and a gift from the Marram Fund.

## References

[1] Horner SM, Vespalcova Z, Lab MJ. Electrode for recording direction of activation, conduction velocity, and monophasic action potential of myocardium. Am. J. Physiol. 1997; 272 (Heart Circ. Physiol. 41): H1917-H1927.

[2] Bayly PV, KenKnight BH, Rogers JM, Hillsley RE, Ideker RE, Smith WM. Estimation of conduction velocity vector fields from epicardial mapping data. IEEE Trans Biomed. Eng..1998;45(5): 563-571.

[3] Kim YH, Garfinkel A, Ikeda T, Wu T, Athill CA, Weiss JN, Karagueuzian HS, Chen PS. Spatiotemporal complexity of ventricular fibrillation revealed by tissue mass reduction in isolated swine right ventricle. J. Clin. Invest. 1997;100 (10):2486-2500.

[4] Malkin RA, Pendley PD. Construction of a very high-density extracellular electrode array. Am. J. Physiol. Heart. Circ. Physiol. 2000;279:H437-H442.

[5] Shors SM, Sahakian AV, Sih HJ, Swiryn S. A method for determining high-resolution activation time delays in unipolar cardiac mapping. IEEE Trans. Biomed. Eng. 1996;43(12):1192-1196.

[6] Hansson A, Holm M, Blomstrom P, Johansson R, Luhrs C, Brandt J, Olsson SB. Right atrial free wall conduction velocity and degree of anisotropy in patients with stable sinus rhythm studied during open heart surgery. Eur. Heart J. 1998;19(2):293-300.

[7] Fast VG, Kleber AG. Role of wavefront curvature in propagation of cardiac impulse. Cardiovasc. Res. 1997;33:258-271.

[8] Joly D, Savard P, Roberge FA, Vermeulen M, Shenasa M. Simulation and experimental studies of the factors influencing the frequency spectrum of cardiac extracellular waveforms. J. Electrocardiol.1990;23(2):109-125.

Address for correspondence

John Triedman, MD
Department of Cardiology, Children's Hospital
300 Longwood Avenue, Boston MA 02115-5724
triedman@cardio1.tch.harvard.edu